NUMERICAL SIMULATION OF MICROCLIMATIC AND ACTIVE LAYER REGIMES IN A HIGH ARCTIC ENVIRONMENT

FINAL REPORT 1974/75

for

DEPARTMENT OF INDIAN AND NORTHERN AFFAIRS
ARCTIC LAND USE RESEARCH PROGRAM

by

M.W. Smith
Department of Geography
Carleton University
Ottawa, Ontario

March, 1975

S-1

NUMERICAL SIMULATION OF MICROCLIMATIC AND ACTIVE LAYER REGIMES IN A HIGH ARCTIC ENVIRONMENT

FINAL REPORT 1974/75

for

DEPARTMENT OF INDIAN AND NORTHERN AFFAIRS

ARCTIC LAND USE RESEARCH PROGRAM

by

M.W. Smith
Department of Geography
Carleton University
Ottawa, Ontario

This report was prepared under contract for the Arctic Land Use Research Program, Northern Natural Resources and Environment Branch, Department of Indian and Northern Affairs. The views, conclusions and recommendations expressed herein are those of the author and not necessarily those of the Department.

March, 1975

TABLE OF CONTENTS

LIST OF FIGURES AND TABLES

FIGURE

TABLE

Abstract

Field data are being gathered to evaluate a computer simulator (Outcalt 1972) which predicts microclimatic and ground thermal regimes using routine weather information and site-specific radiative, aerodynamic, thermal and hydrologic characteristics. From these data the model synthesizes the local surface energy budget and the surface temperature which is used as the boundary condition in the soil thermal diffusion equation. The predictive capability can be used as a basis for land use decisions.

Field measurements of energy budget components and ground temperatures are being used to test the accuracy of predictions. Two natural sites, one wet and one dry, near Eureka, N.W.T., have been fully instrumented. At another two disturbed sites ground temperatures are being measured.

The spring snowmelt event is very well duplicated by the model with predictions closely matching the observations for the start and finish of melt. Active layer thicknesses reach a maximum in mid-August, with mean values of 30 cm at the wet site and 52 cm at the dry site. The model predictions are 29 cm and 53 cm respectively, also by mid-August. The pattern of freeze-back is also well duplicated. The zero-curtain period lasts for about four weeks at the wet site but less than two weeks at the dry site. The predicted sequences match this fairly well, except that they lag by about five days throughout. Removal in July 1973 of a 10-cm surface layer at the wet site led to a 10-cm thickening of the active layer in mid-August. Simulation of this disturbance yielded an almost identical result. The effects of winter snow compaction were also investigated through simulation, the results showing that there is neglibile carry-over effect on summer ground temperatures.

Model predictions of mean daily net radiation under naturally cloudy skies are within 5% of observed values.

1. Introduction

Work began in 1973 on a program of field study and computer simulation of microclimatic and ground thermal regime in a high arctic location near Eureka, N.W.T.

The study is concerned with the development of a generalized predictive model which could be used to estimate the expected magnitude of microclimatic and subsurface thermal disturbances associated with various types of exploration and development activity. Approximately 2.5 million km^2 of Canada is tundra, with about 1.4 million km^2 comprising the Archipelago. In such a vast area there is a great range in climatic and microclimatic conditions. Empirical studies that are carried out are often valid for only small portions of this large area and there is thus a need to develop generalized (theoretically-based) strategies for the solution of environmental problems.

Logistical problems limited progress in 1973 but field work was more successful during 1974. This report covers the results of this research, undertaken as part of the Arctic Land Use Research (ALUR) program of the Department of Indian and Northern Affairs.

In addition to the Department of Indian and Northern Affairs, I would like to thank the following agencies and individuals. The Polar Continental Shelf Project for aircraft support, field supplies, accommodation and communications; the Atmospheric Environment Service at Eureka, N.W.T.; Bradley Air Services at Eureka; Mr. D.M. Hodgson, Terrain Sciences Division, Geological Survey of Canada for drilling boreholes and logistical help; Dr. S.I. Outcalt, Department of Geography, University of Michigan, for copies of some of his computer programs; and D. Hiscocks, C. Hotzel, R. Miller and D. Moxley for their assistance in field work.

2. Objectives

The objectives of this study, to be accomplished through energy balance studies of natural and disturbed sites in a high arctic environment, are to:

1) Obtain an understanding of the natural system

2) Test a computer model which can predict microclimatic and active layer regimes using routine climate data collected by the Atmospheric Environment Service.

Using a generalized modelling approach, one can investigate the short- and long-term, delayed and persistent effects of human activity in a way that is impractical through field experimentation. Typical problems that might be analyzed include the removal of surface layers, compaction of surface layers and snow cover, construction and insulation of pipelines and roads, etc. If results from simulation are shown to agree with nature satisfactorily, it would then offer solutions to numerous engineering decisions that are traditionally made on the basis of intuition and experience - a procedure which is hazardous where experience is limited. The predictive capability can further be used as a basis for land use decisions.

Active layer development is the most important feature of the thermal regime in arctic regions and attention has been focussed upon this, together with the snowmelt and freeze-back events. The simulator can further be used to determine the mean and extreme dates of these critical events.

With this in mind, the particular aspects of the model being examined most critically are the predictions of:

1) The snowmelt event, which marks the beginning of the thaw period

2) Active layer development

3) Freeze-back of the active layer.

In addition, the accuracy of these predictions must be checked in the context of the overall consistency of the model - i.e., how well the radiation and energy regimes are themselves duplicated. In this way the physical integrity of the model is evaluated, which is important in assuring spatial and temporal generality.

3. Summary of Activities

The main activity during the summers of 1973 and 1974 was the establishment and instrumentation of field sites. Detailed information is needed to corroborate simulator performance and all input and output parameters are being measured. These include the components of the surface energy regime and the ground thermal regime. In this way model performance can be evaluated, developed and improved.

3.1 Field Sites

A location in the vicinity of Eureka, Ellesmere Island, N.W.T. was selected for detailed field investigations. Following field reconnaissance, an area was selected on the Fosheim Peninsula about 20 km north of Eureka (Figure 1). A number of terrain units have been identified in this area (Inglis and Jonkel 1973, Lambert 1974) and two of these were selected for detailed investigations on the basis that they typify the extremes in surface conditions and hence in microclimatic and ground thermal regimes:

i) Site 1 - Low-centred polygons, impeded drainage, some standing water, soil moisture contents in the range of 70-400% by dry weight. Moss cover is about 90% and the site is dominated by a meadow-type vegetation with *Carex stans* dominant (Lambert, 1974). The soil profile has a definite organic layer up to 10 cm thick which overlies a silty-clay layer about 20 cm thick. Below this to 3 m it is mostly ice.

ii) Site 2 - *Salix-Dryas* plain (Inglis and Jonkel 1973), which exhibits gradation from small (1 to 1.5 m diameter), high-centred polygons to earth hummocks. The ground is dry, with soil moisture contents in the range of 10-30% dry weight. The vegetation cover is only about 20-30% (Lambert 1974). Soils are undifferentiated and consist of a silty-sand with some rock flour.

Vegetation characteristics are summarized in Table 1. The two sites are in juxtaposition and on fairly level terrain (Figure 2). Fetch distances are limited to 100-150 m. Three-meter boreholes were drilled at each site[1] and the cores recovered for determination of physical properties (Table 2).

---

[1] This was carried out by D.M. Hodgson, Terrain Sciences Division, Geological Survey of Canada.

It is reasonable to assume that there are no macroclimatic differences between these two sites and that two different microclimates are a result of the difference in surface and subsurface properties which alter the components of the energy balance. Availability of data on two microclimates within the same macroclimate permits more effective testing of the computer model.

In addition to these natural sites, two sites which had been disturbed for experimental reasons (see Lambert 1974) were instrumented for ground temperatures. These sites are in the same two terrain units as above, with the surface material removed down to the active layer in July, 1973.

4. Theory and Instrumentation

Each site has been fully instrumented for energy balance studies. The Bowen Ratio approach was selected as being the most appropriate for determination of energy balance components. This approach has proven reliable in many previous studies (e.g., Rouse and Kershaw 1971, Davies and Allen 1973) and is preferred over the aerodynamic method (see Gray et al. 1974).

The energy balance equation is given by:

$$Rn = H + LE + G \tag{1}$$

where Rn is net radiation, H is the convective transfer of heat into the air, LE is the energy used for evaporation, and G is the conduction of heat into the ground. Both Rn and G can be measured directly quite easily - values for H and LE are obtained through re-arranging equation (1) to read

$$H + LE = Rn - G \tag{2}$$

or by dividng LE,

$$LE = \frac{Rn - G}{1 + H/LE} = \frac{Rn - G}{1 + B} \tag{3}$$

where B = H/LE and is known as the Bowen Ratio. Once B is determined then values for LE and H are easily obtained. Now, if air temperature (T) is measured at two heights above the surface to give ΔT, and the vapour pressure (e) is measured at the same two heights to give Δe, then,

$$B = \gamma \frac{\Delta T}{\Delta e} \tag{4}$$

where γ is the psychrometric constant. Thus simultaneous measurements of R_n, G, ΔT and Δe permit the determination of the surface energy balance components. This method is well suited to values averaged over half-hourly or hourly intervals.

In the measurement program net radiation (R_n) is being measured with a Funk net radiometer (Swissteco, Type S-1), at a height of 1 m above the surface. Resolution is ± 0.02 mW cm^{-2}. Incoming solar radiation (R_s) is measured with a Kipp solarimeter, and inverted solarimeters measure albedo (α) at each site. Ground heat flux (G) is being measured using three heat flux plates (Middleton) in series at each site, also with a resolution of ± 0.02 mW cm^{-2}. The plates are buried at a depth of 5 cm and the flux divergence between here and the surface is determined from temperature measurements. Air temperatures are being measured at three levels (25, 75 and 150 cm) with thermocouples housed in naturally-aspirated radiation shields; accuracy is within ± 0.1^{o}C. The humidity profile is being measured with electrical resistance sensors (Phys-Chem Research, PCRC-11). These are accurate to within ± 1% relative humidity. The components of the measurement system are shown in Figure 3. A two-meter tower was erected at each site. For the ground thermal regime, temperature cables were installed with thermocouples extending from the ground surface down to 3 m (Figure 3). Regular determinations of soil moisture are also carried out when the ground is unfrozen.

Macroclimatic data required by the simulator are being provided by the Atmospheric Environment Service at Eureka and from a 15-meter tower, instrumented for temperature, humidity and windspeed profiles and incoming solar radiation located at the field site (Figure 2). Unfortunately this tower arrived too late for installation in 1973 but was put into operation in July, 1974.

4.1 Data Collection and Handling

A total of 70 meteorological variables are digitally recorded on two magnetic tape cassette recorders[2]. These recorders have very low power requirements and will run for extended periods on heavy-duty 12-volt automobile batteries (Figure 4).

Cables from the meteorological sensors are all led into a hut, which contains a small propane-heated enclosure, which is designed to allow the recorder to run unattended through the winter months. The recorder enclosure is set into the ground and is insulated with one-foot thick styrofoam on all sides.

The magnetic tapes can be easily transcribed into computer-compatible format, and the data can then be quickly available and ready for analysis.

5. The Computer Model

Most efforts to develop mathematical-predictive models of ground thermal regime have employed the surface temperature or heat flux as a prescribed boundary condition (e.g. Lachenbruch 1959; Nakano and Brown 1972). In reality the surface thermal regime is an expression of the microclimate which itself results from the interaction of local weather and the site-specific aerodynamic, radiative and thermal properties, and hydrologic conditions that affect energy exchange. This interaction determines the magnitude of the individual components of the surface energy balance.

The value of the energy balance approach to understanding permafrost problems has been advocated by Benninghoff (1963) and Brown (1963, 1965). Gray et al. (1974) point out that since every change that man makes to the natural terrain alters the surface heat exchange and the ground thermal regime, the energy balance is an appropriate approach within which to quantify the effects of these changes.

---

[2] The recorders are the ADR-II, Sander Geophysics, Ottawa, Ontario.

A suitable generalized strategy for ground thermal problems is one in which the surface energy balance is modelled in order to derive the boundary conditions governing the subsurface regime. Ground temperatures are thus explicitly linked to the microclimate which makes it possible to relate spatial and temporal variation to specific site characteristics. Such a strategy is more realistic and preferable to those in which ground temperatures are forced by some specified surface regime, since surface temperature is highly variable both spatially and temporally with extrapolation being difficult.

Energy balance models have been developed by Myrup (1969), Outcalt (1971, 1972) and Goodwin (1972). Goodrich (1974) has also incorporated energy balance considerations into a geothermal model.

A model developed by Outcalt (1972) synthesizes the surface energy balance from standard climatological data, such as that collected by the Atmospheric Environment Service. The computer simulator predicts the component fluxes of the surface energy balance - net radiation, evaporation, convection, ground heat conduction - as well as the surface temperature. The surface temperature is then used as the boundary condition, together with the details of ground thermal properties, to produce the ground temperature field. The energetics of freezing and thawing are incorporated. The model design is shown diagrammatically in Figure 5 .

The station network of the Atmospheric Environment Service collects regional climatic data. The local climate of any place, termed the microclimate, results from the interaction of this regional climate with certain local factors. The simulator accommodates the interaction of these two sets of factors which comprise:

1) Regional weather data - air temperature (T_a) humidity (q_a), incoming solar radiation (R_s), cloud cover (n) and type (k), wind speed (u), snow depth, and atmospheric pressure.

2) Site specific properties - aerodynamic roughness, albedo, per cent surface saturation, ground thermal properties (conductivity, heat capacity). An estimate of the mean annual ground temperature at the depth of zero amplitude is also required. Site data can be varied seasonally as appropriate.

The computational method is based upon the energy conservation equation,

$$R_n = H + LE + G \tag{5}$$

or,

$$R_n + H + LE + G = 0 \tag{6}$$

(ignoring signs) - i.e., the components of surface energy transfer must have an instantaneous zero sum. Each component can be expressed in terms of the surface temperature, as follows:

i) $$R_n = R_s\ (1 - \alpha) + R_L{\downarrow} - \varepsilon\sigma\, T_s^{\,4} \tag{7}$$

where $R_L{\downarrow}$ is the incoming longwave radiation from the atmosphere, ε is the surface emissivity, σ is the Stefan-Boltzmann constant and T_s is the surface temperature. Following Idso and Jackson (1969) and Sellers (1965), the net longwave balance at the surface, under cloudy skies, is given by:

$$R_L{\downarrow} - \varepsilon\sigma\, T_s^{\,4} = \left[\varepsilon\sigma\, T_a^{\,4}\ \left(1 - c\ \exp\left(-d\,(T_a - 273)^2\right)\right) - \varepsilon\sigma\, T_s^{\,4}\right] \times \left[1 - kn^m\right] \tag{8}$$

where T_a is the air temperature, c and d are constants, n is cloud cover (in tenths), k is a coefficient depending on cloud type and m is an exponent (a value of 2 is used here - see Sellers, p. 61).

ii) $$H = -\rho c_p\ K_h\ \frac{(T_s - T_a)}{\Delta z} \tag{9}$$

where ρ is the density of air, c_p the specific heat, K_h is a turbulent transfer coefficient for heat and Δz is the difference in height between T_s and T_a.

iii) $$LE = -\rho L K_w \frac{(q_s - q_a)}{\Delta z} \tag{10}$$

where L is the latent heat of vapourization, K_w a turbulent transfer coefficient for water vapour and q is the specific humidity. The surface humidity, q_s, is a function of the surface temperature, T_s.

iv) $$G = -\frac{K (T_s - T_z)}{\Delta z} \tag{11}$$

where K is the thermal conductivity of the ground and T_z the temperature at some depth z.

When atmospheric, surface and subsurface variables are specified at some instant (e.g., minute, hour, day), the surface temperature has a unique value - the equilibrium surface temperature (Outcalt 1972). The computational procedure determines this and the energy balance components. The Businger-Dyer diabatic wind profile is used to determine K_h (Paulson 1970, Goodwin 1972) and the Bowen Ratio is then used for LE. Ground temperatures are calculated using the finite-difference form of the thermal diffusion equation at a node-spacing of 5 cm.

Since the computer program is still undergoing development, a copy is not made available at this time but will be included in the final report in 1976.

6. Results

6.1 Site 1 (Wet)

The ground at this site is composed of three distinct layers: organic matter up to 10 cm thick, clayey-silt about 20 cm thick and then mostly pure ice. Physical and thermal properties of these layers are summarized in Table 3. The surface organic layer is quite similar to that described by Nakano and Brown (1972) and their thermal conductivity values have been used here, since experimental determinations are particularly difficult for such materials. The thermal conductivities for other layers were calculated using the equations of Kersten (1949). The frozen and unfrozen heat capacities were determined from physical data using the method of de Vries (1963). It is recognized that unfrozen water persists at temperatures below $0^{\circ}C$, and that this has a great effect on the energetics of freeze-thaw. In the present application of the model it is assumed that phase change takes place over a range of temperature which depends on the soil type (e.g., Williams 1968). Ideally, data should be available on the unfrozen water content as a function of the soil temperature, which could easily be incorporated into the model. This is planned for the future.

Other input data are also summarized in Table 3.

In all the following sections 1974 daily weather data for Eureka were used in the model, allowing direct comparison of actual and predicted situations.

6.1.1 Snowmelt

The sequence of events during snowmelt is very well duplicated in the model. The predicted start of snowmelt on June 20 exactly coincides with observations in the field. The model predicts that snowmelt was completed by June 22, which is just slightly earlier than the actual date (June 24). The snowmelt predictions are thus very good.

One of the most important aspects of tundra snowmelt is the progressive reduction in albedo as more and more of the underlying surface becomes exposed. As the snow surface has an albedo close to 0.8 and the tundra surface near 0.2, the proportion of exposed ground has a great effect on the amount of solar radiation absorbed. Because of the uneven distribution of snow cover on the Fosheim, snow-free patches of tundra appear quite early during the snowmelt period. These bare patches heat up quickly and warm air advection to the remaining snow-covered areas hastens the snowelt process (cf. Weller et al. 1972). Thus surface albedo must be expressed as some function of snow depth; this was done in accordance with field data of Weller et al. (p. 296). Since the predicted snowmelt is faster than the actual, the albedo function may require modification. This will be tested in Spring, 1975.

Thaw initiation follows immediately after snowmelt.

6.1.2 Active Layer Development

High soil water contents, which promote evaporative cooling at the surface and a large latent heat effect, mean that the wet site has the shallowest active layer of any site in the area. The predicted maximum depth of thaw of 29 cm (on August 16) is in excellent agreement with that actually measured in the field (30 cm). In 1973 the maximum was 29 cm, indicating that active layer thickness is a conservative parameter. The dates of the maxima were mid-August in all cases. The predicted pattern of active layer development is not entirely satisfactory (Figure This is not quite so serious as it might appear since the predicted 20-cm temperature during the period July 22 to August 5 was close to thawing, between -1.0 to -0.5°C. However, it does seem that the thermal conductivity value for the unfrozen surface organic layer is too low. The predicted pattern when this layer is removed (Figure 6) does more closely resemble the observed pattern of development.

The slight difference at the beginning of the thaw season (Figure 6) is due to the predicted snowmelt being completed two days earlier than the actual.

6.1.3 Freeze-Back

The main feature of the freeze-back in permafrost regions is the zero-curtain phenomenon where, due to the release of latent heat of fusion, the active layer remains close to 0°C for a prolonged period of time. This is important, since during this period the ground will not be completely mechanically frozen. Thus any model should be capable of duplicating this zero-curtain phenomenon.

Observations showed that this period lasted about four weeks (August 27 - September 22) at the wet site where there is much water to be frozen. During this time the 20-cm temperature hovered around -0.2 to -0.3°C (Figure 7). Predicted values agree very closely with observations and although they are a little colder this is considered minor in comparison with the excellent correspondence in the overall freeze-back sequence. The zero-curtain period is terminated, when all the water has finally frozen, by a very sharp drop in temperature. This also is well duplicated in the model, although just a few days late (Figure 7).

6.1.4 Effects of Surface Disturbance

6.1.4.1 Removal of Surface Layer

Removal of 10 cm of organic material on July 15 led to a predicted active layer thickness of 41 cm below the original surface by August 16 (Figure 6). This result agrees almost exactly with field measurements of 40 cm in August, 1974 and 44 cm in 1973 (Lambert 1974) following controlled field disturbance. The model thus provides a reasonable estimate of the effect of surface disturbance on permafrost. Since the ground below 30 cm is mostly ice, severe thermokarst problems would result.

6.1.4.2 Snow Cover Compaction

The effects of snow compaction, such as could be due to winter operations, were examined through simulation. It is possible that compaction of the snow cover, by reducing the insulation afforded the soil in winter, may affect plant viability in the following summer.

As an extreme case the snow was assumed compacted by 20% (a figure taken from snowmobile studies - G. Merriam, personal communication[3]). Ground temperatures, although colder in winter, were found to warm up more quickly during spring (prior to snowmelt) due to the increased thermal conductivity of the snow cover. The net result was that there was virtually no effect on the final active layer depth, which reached 28 cm by

[3] Dr. G. Merriam, Department of Biology, Carleton University, Ottawa.

mid-August. The conclusion is that root-zone temperatures would in fact be similar to those in an undisturbed site and there would be no effect on vegetation.

6.2 Site 2 (Dry)

The snowmelt event is assumed to be the same as at Site 1. The small differences in snow depth at this site caused little variation from the melt pattern observed at Site 1.

6.2.1 Active Layer Development

Active layer thicknesses are greater at dry sites because the much reduced evaporation promotes higher surface temperatures. Also latent heat effects are not so great and the $0^{o}C$ isotherm penetrates the ground more quickly.

There is more difficulty in specifying the surface wetness for 'dry' sites. This factor, which is assumed equivalent to the percentage saturation of the surface soil layer (0-5 cm), is quite variable in the field both spatially and temporally. From daily measurements of surface soil moisture contents, a wetness of 50-60% is representative for Site 2 (Figure 8). In spot locations at different times around the site, wetness is as low as 15% and as high as 100%. It is clearly not as uniform, hydrologically, as Site 1. In future tests of the model the surface wetness will be specified on a daily basis during the summer period, allowing comparison with results when an average value is used.

Inputs to the model for Site 2 are listed in Table 4. The dryness of the site leads to higher surface and subsurface temperatures than at Site 1. Measurements of surface temperatures (using a Barnes PRT-10 IR thermometer) at the two sites on July 22-23 gave mean daily values of $11.0^{o}C$ and $8.0^{o}C$. This compares to predicted values of 9.3^{o} and $7.1^{o}C$ from the model.

The model predicts that, by mid-August, the frost table reaches 53 cm. Field measurements of active layer thickness show it to be quite variable around this site, ranging from 44 to 65 cm with a mean depth of

52.5 cm (s.d. = ± 6.0 cm). The model result is thus in very good agreement with the mean value. The pattern of development is also well reproduced in the model results (Figure 6).

6.2.2 Freeze-Back

Because there is much less soil moisture to freeze at Site 2, the zero-curtain period is shorter, lasting only about 10 days (Figure 7). As with the wet site, the overall trend is again reproduced quite well, except that the predicted pattern lages by a few days. The observed and predicted dates of final freeze-up (i.e., when the temperature starts to fall quickly) are September 10 and September 15 respectively. This error is about the same as at Site 1.

6.3 Net Radiation

As a preliminary evaluation of the physical integrity of the foregoing results, a comparison of observed and predicted values for the net radiation has been made. The observed values are those for the Eureka weather station, whose radiation site is quite similar to the dry field site. Values for the snow-free period (July-August) only are compared because of the uncertainty of specific surface conditions at Eureka at other times.

The two sets of values are shown in Figure 9 and the agreement is very good. There are certainly some large deviations on a few days, but on a monthly basis the two sets of values are within 5%. The mean daily values for July are 249 ly/day (observed) and 260 ly/day; for August they are 92 and 93 ly/day.

7. Conclusions

The results so far indicate that the numerical model performs well in a variety of predictions. This includes dates as well as actual magnitudes. More critical testing, in terms of energy balance components, is still being carried out and will be reported on in the future.

Some specific conclusions reached so far include:

1) The predicted date of snowmelt (June 20) is in excellent agreement with field observations (June 20), although the predicted completion of melt is earlier than that which actually occurred (June 22 vs. June 24).

2) The predicted maximum depths of thaw at the wet and dry sites of 29 and 53 cm respectively are in close agreement with the field measurements of 30 and 52 cm. There is some disagreement in the pattern of active layer development, particularly at the wet site where the thermal conductivity value may be in error.

3) The freeze-back event at both sites is well duplicated in the model. The duration of the zero-curtain effect is essentially correct in both cases, although predicted specific dates are about five days late.

4) Simulation of the removal of the surface organic layer gave results in excellent agreement with observations. This indicates that the model should be capable of yielding accurate predictions of the effects of surface disturbance. Simulation of snow compaction due to winter operations shows that there should be no detrimental thermal effects in the plant root zone in the following summer.

5) Observed and predicted values for net radiation for July and August agree within 5% on a mean daily basis.

BIBLIOGRAPHY

Benninghoff, W.S., 1963, "Relationships between vegetation and frost in soils" Proc. Permafrost Inter. Conf., NAS-NRC Publ. 1287, Washington, D.C. pp 9-13.

Brown, R.J.E., 1963, "Influence of vegetation on permafrost", Proc. Permafrost Inter. Conf., NAS-NAC Publ. 1287, Washington, D.C., pp. 20-25.

---------, 1965, "Some observations of the influence of climatic and terrain features on permafrost at Norman Wells, N.W.T., Canada", Can. J. Earth Sci., 2, pp. 15-31.

Davies, J.A. and C.D. Allen, 1973, "Equilibrium, potential and actual evaporation from cropped surfaces in southern Ontario", Jnl. Appl. Met., 12, pp. 649-657.

Goodrich, L.E., 1974, "A one-dimensional numerical model for geothermal problems", NRCC, Technical Paper 421, 22 p. and figures.

Goodwin, C.W., 1972, An annual active-layer simulator for permafrost regions, M.Sc. Thesis, Dept. of Geography, Univ. of Michigan, 71 p.

Gray, D.M., D.E.L. Erikson and F. Abbey, 1974, "Energy studies in an arctic environment", Environmental-Social Committee, Northern Pipelines, Report No. 74-18, 60 p.

Idso, S.B. and R.D. Jackson, 1969, "Thermal radiation from the atmosphere", Jnl. Geophys. Res., 74, pp. 5397-5403.

Inglis, J. and C. Jonkel, 1973, "Ellesmere Island Range Studies", Canadian Wildlife Service Eastern Region, 24 p. and figures.

Kersten, M.S., 1949, Laboratory research for the determination of the thermal properties of soils, Bull. 28, Univ. of Minnesota, Inst. of Tech., Eng. Expt. Stn., 227 p.

Lachenbruch, A.H., 1959, "Periodic heat flow in a stratified medium with application to permafrost problems", U.S. Geol. Survey, Bull. 1083-A, 36 p.

Lambert, J.D.H., 1974, "Botanical studies of natural and manipulated terrain units on the Fosheim Peninsula, Northern Ellesemere Island, N.W.T.", DINA, ALUR Report.

Myrup, L.O., 1969, "A numerical model of the urban heat island", Jnl. Appl. Met., 8, pp. 908 -918.

Nakano, Y. and J. Brown, 1972, "Mathematical modelling and validation of the thermal regimes in tundra soils, Barrow, Alaska", Arctic and Alpine Res., 4, pp. 19-38.

Outcalt, S.I., 1971, "A numerical surface climate simulator", Geog. Analysis, 3, pp. 379-392.

-----------, 1972, "The development and application of a simple digital surface climate simulator", Jnl. Appl. Met., 11, pp. 629-656.

Paulson, C.A., 1970, "The mathematical representation of wind speed and temperature profiles in the unstable atmospheric surface layer", Jnl. Appl. Met., 9, pp. 857-861.

Rouse, W.R. and K.A. Kershaw, 1971, "The effects of burning on the heat and water regimes of lichen-dominated subarctic surfaces", Arctic and Alpine Res., 3, pp. 291-304.

Sellers, W.D., 1965, Physical Climatology, Univ. of Chicago Press, 272 p.

Vries, D.A. de, 1963, "Thermal properties of soils", Physics of Plant Environment, W.R. van Wijk, ed., North Holland Publ. Co., pp. 210-235.

Weller, G., et al., 1972, "The tundra microclimate during snow melt at Barrow, Alaska", Arctic, 25, pp. 291-300.

---------- and B. Holmgren, 1974, "The microclimates of the Arctic tundra", Jnl. Appl. Met., 13, pp. 854-862.

Williams, P.J., 1968, Properties and behaviour of freezing soils, NRCC Research Paper No. 259, 119 p.

FIGURE 1

LOCATION OF STUDY AREA

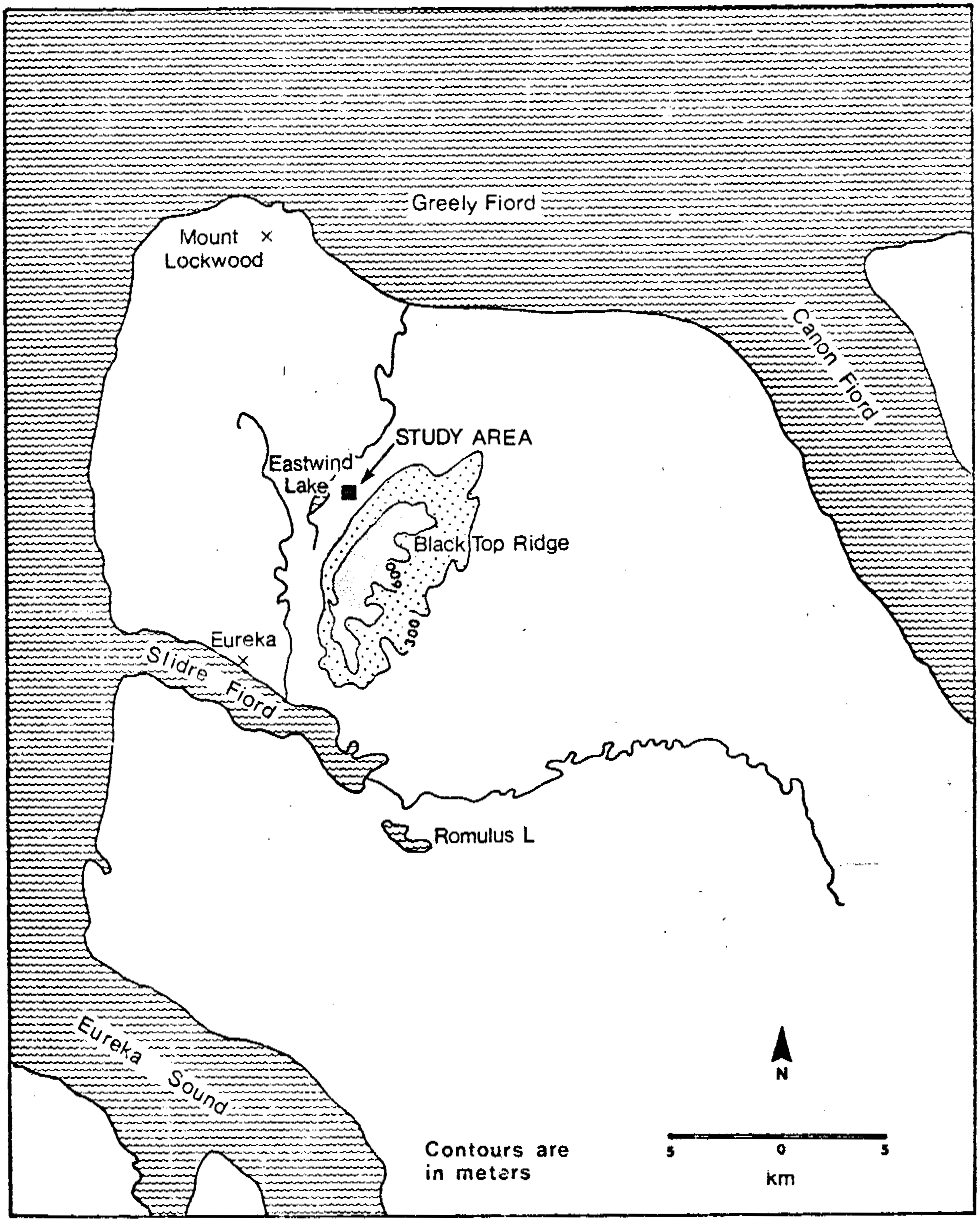

FIGURE 2

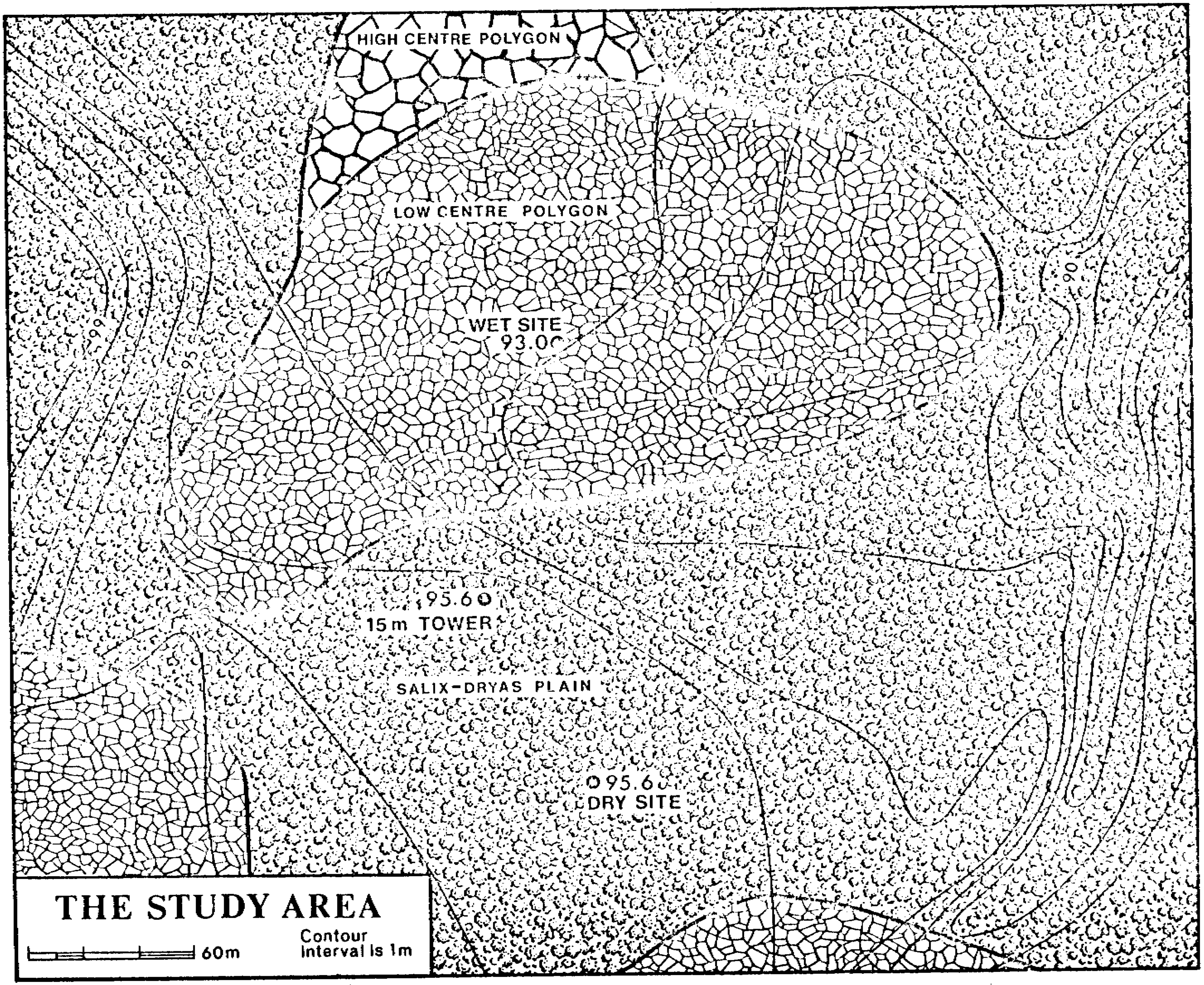
HIGH CENTRE POLYGON
LOW CENTRE POLYGON
WET SITE
93.00
99
95
90
95.60
15m TOWER
SALIX-DRYAS PLAIN
95.6
DRY SITE
THE STUDY AREA
60m
Contour
interval is 1m

FIGURE 3

INSTRUMENTATION AT MICROCLIMATIC SITES

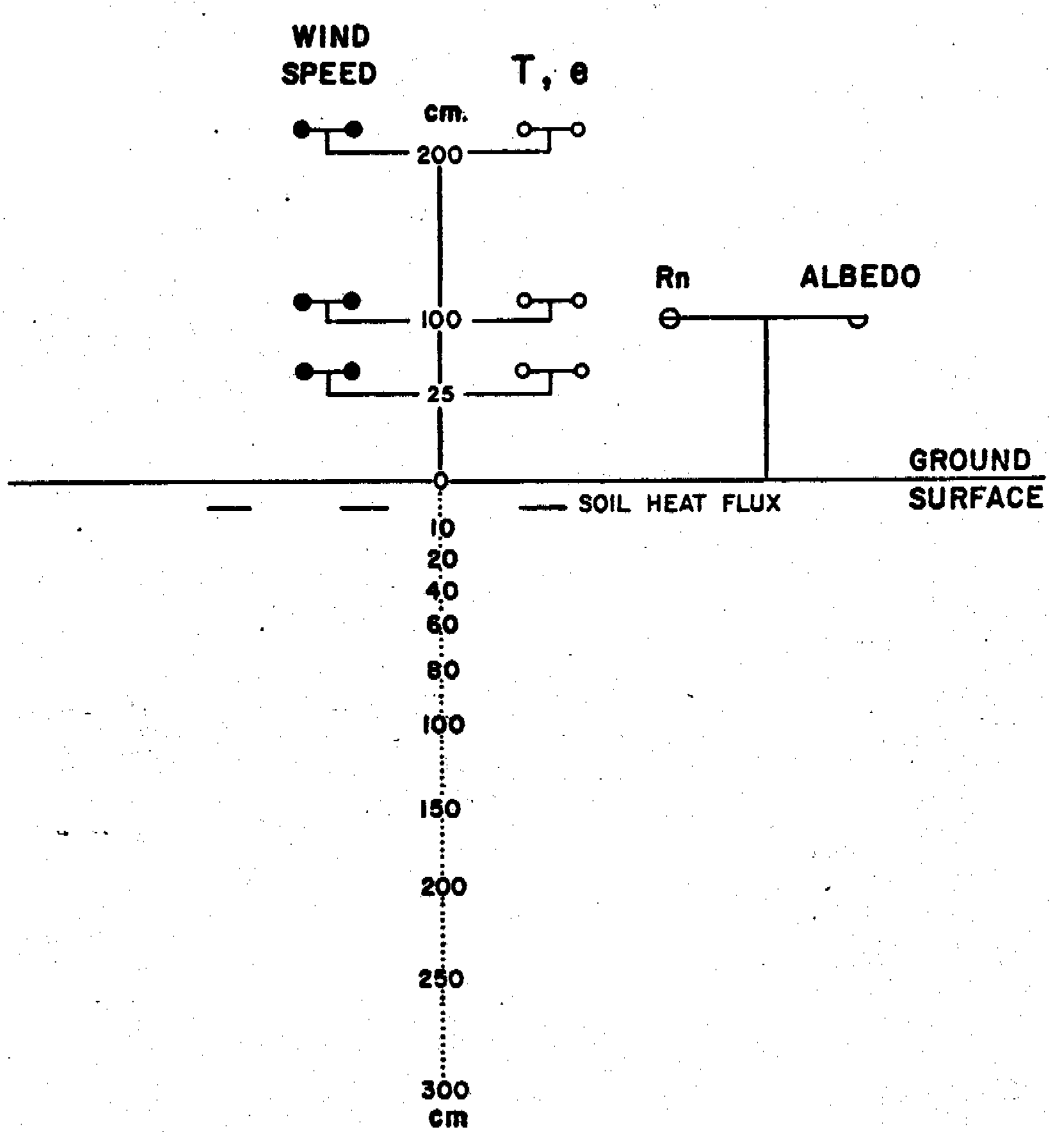

FIGURE 5

PROGRAM FLOW CHART

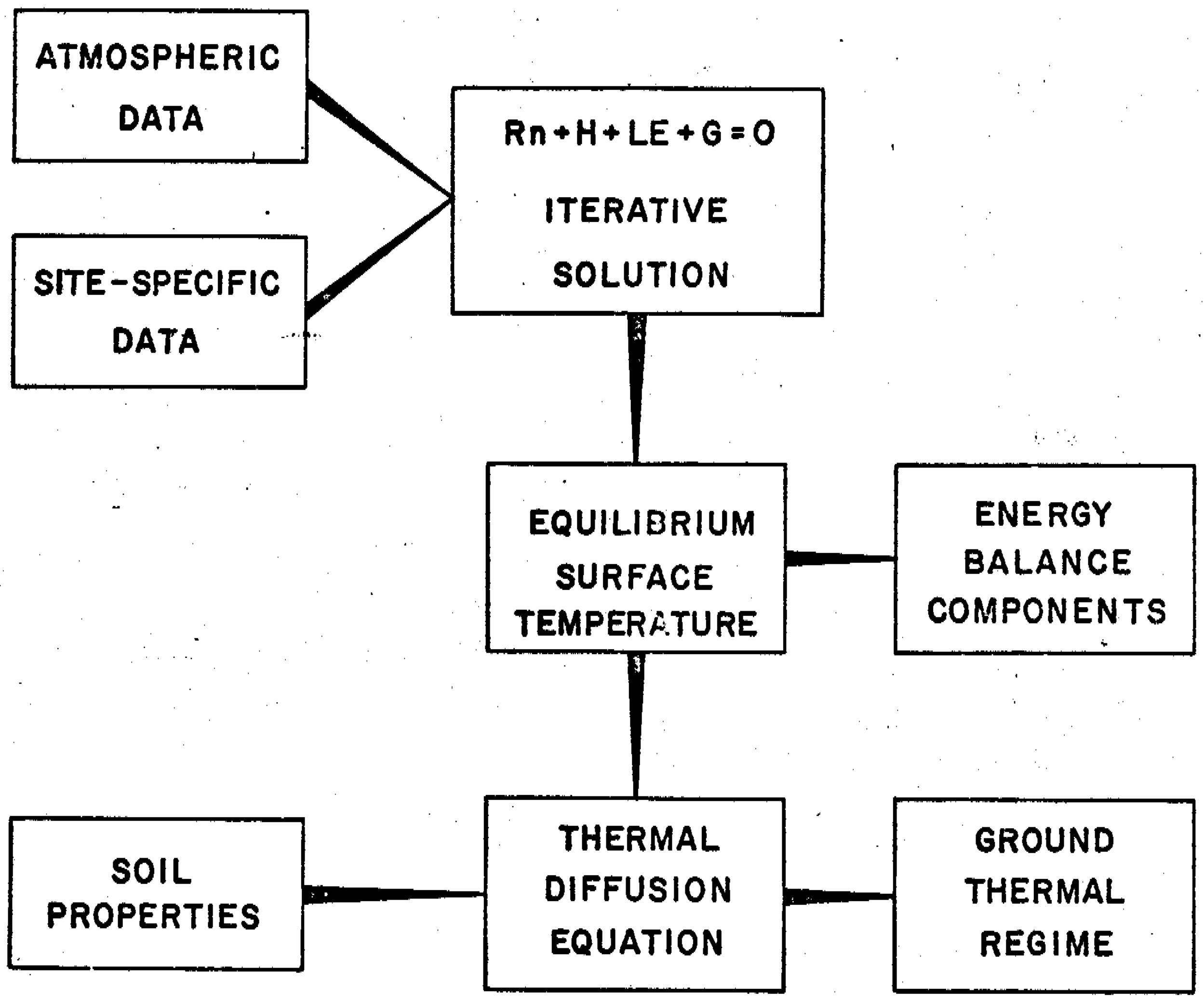

FIGURE 6

ACTIVE LAYER DEVELOPMENT - OBSERVED AND PREDICTED

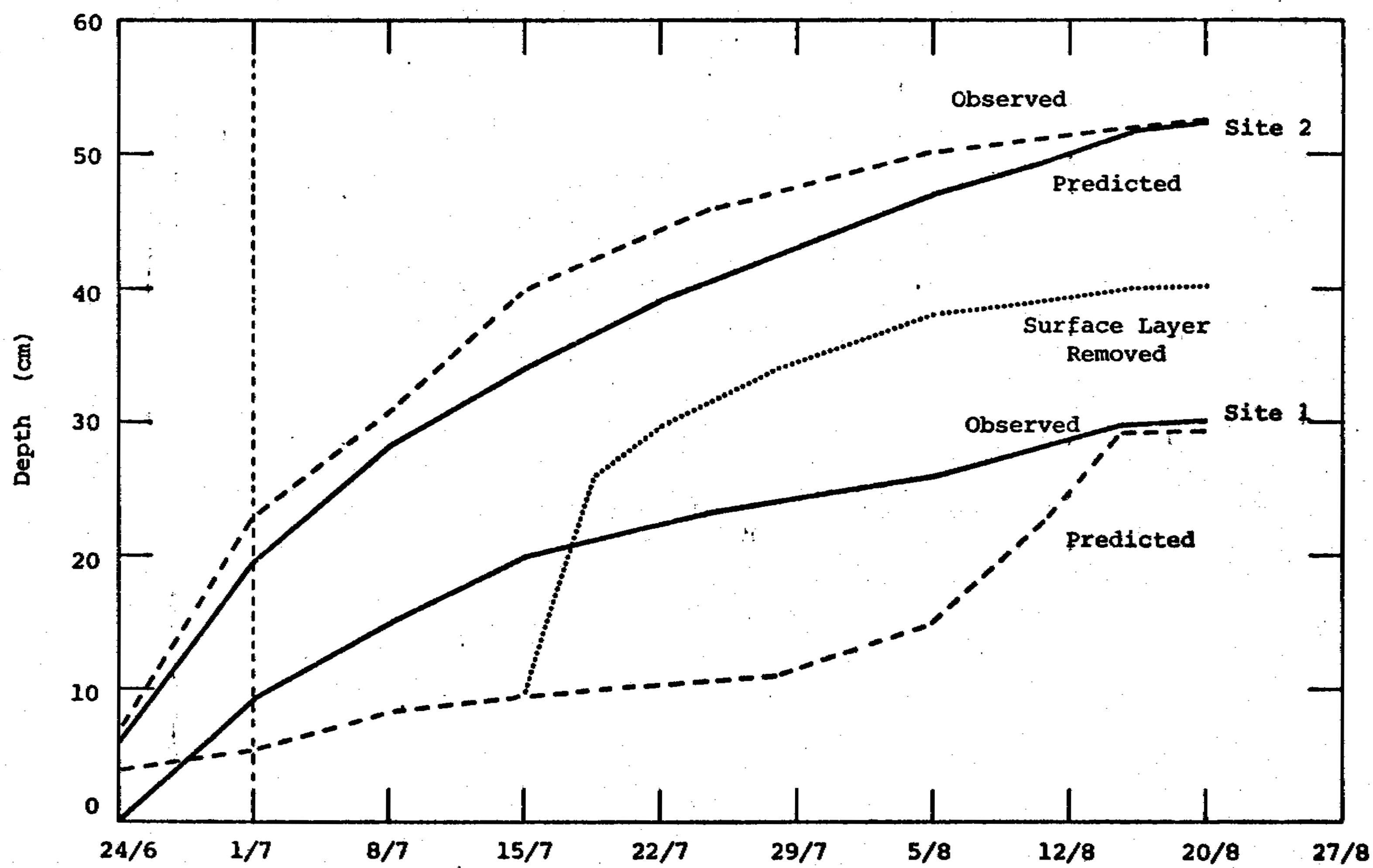

FIGURE 7 - FREEZE-BACK TEMPERATURES - OBSERVED AND PREDICTED

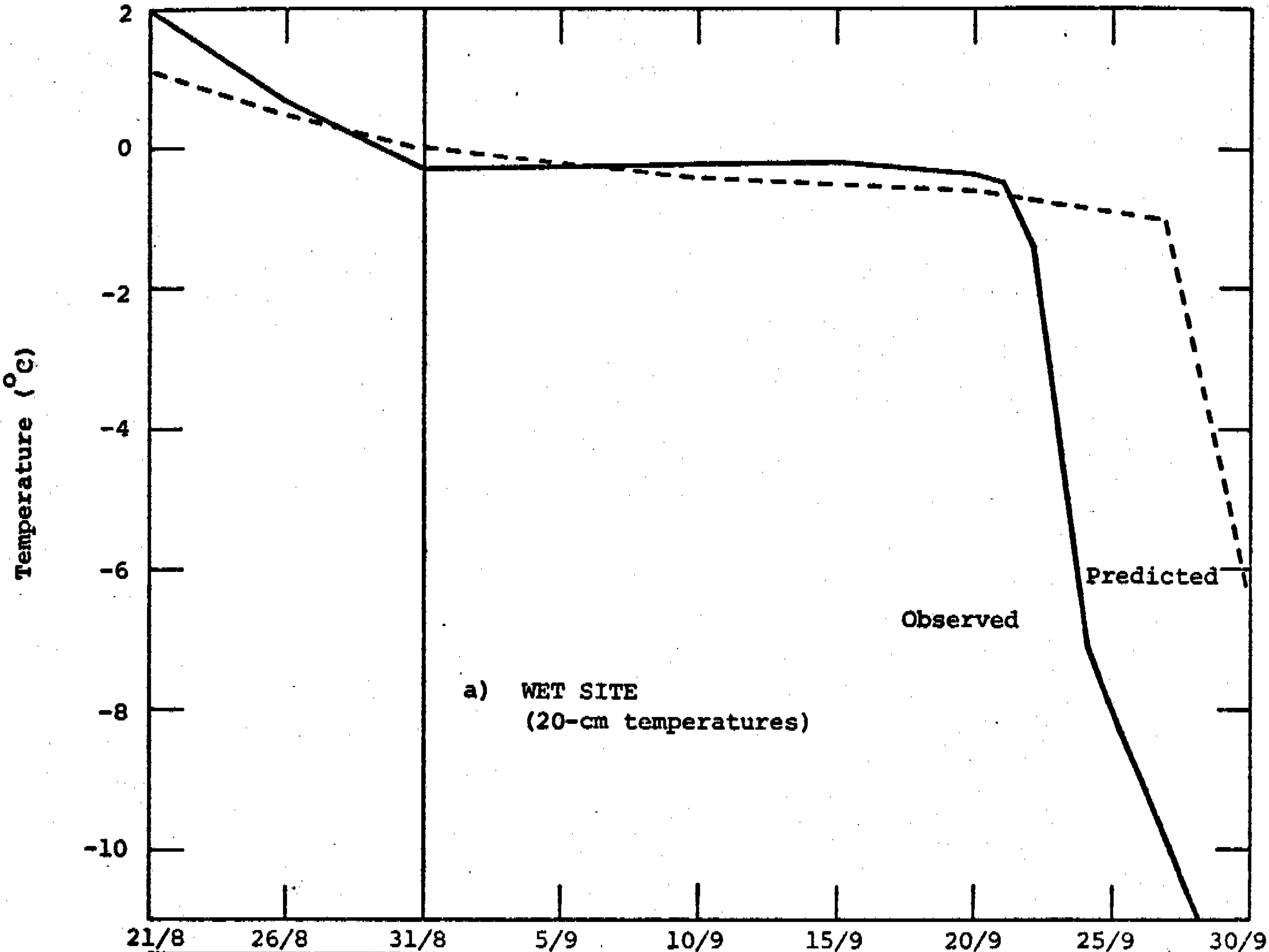

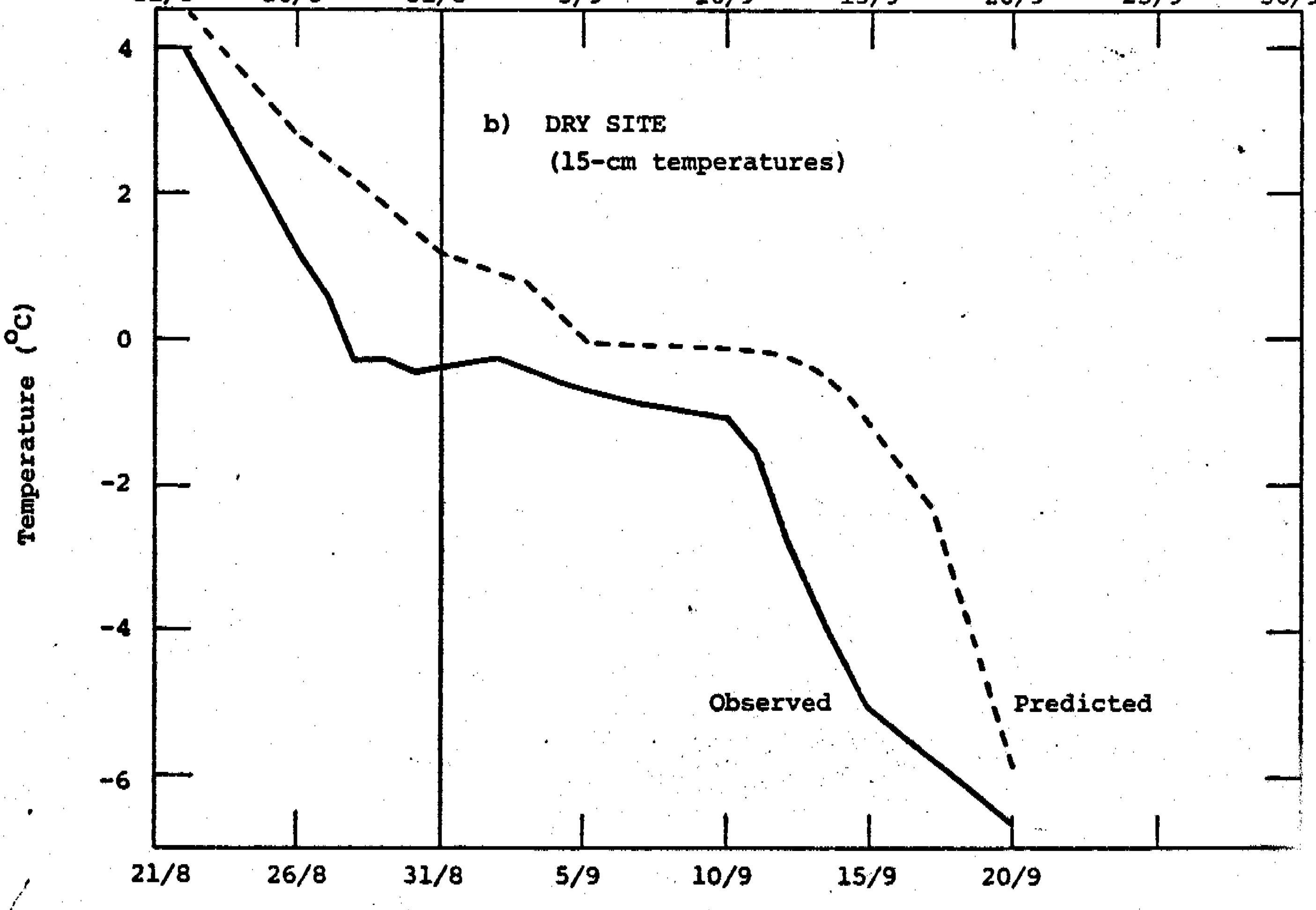

FIGURE 8

VARIATIONS IN SOIL MOISTURE AT SITE 2 (DRY)

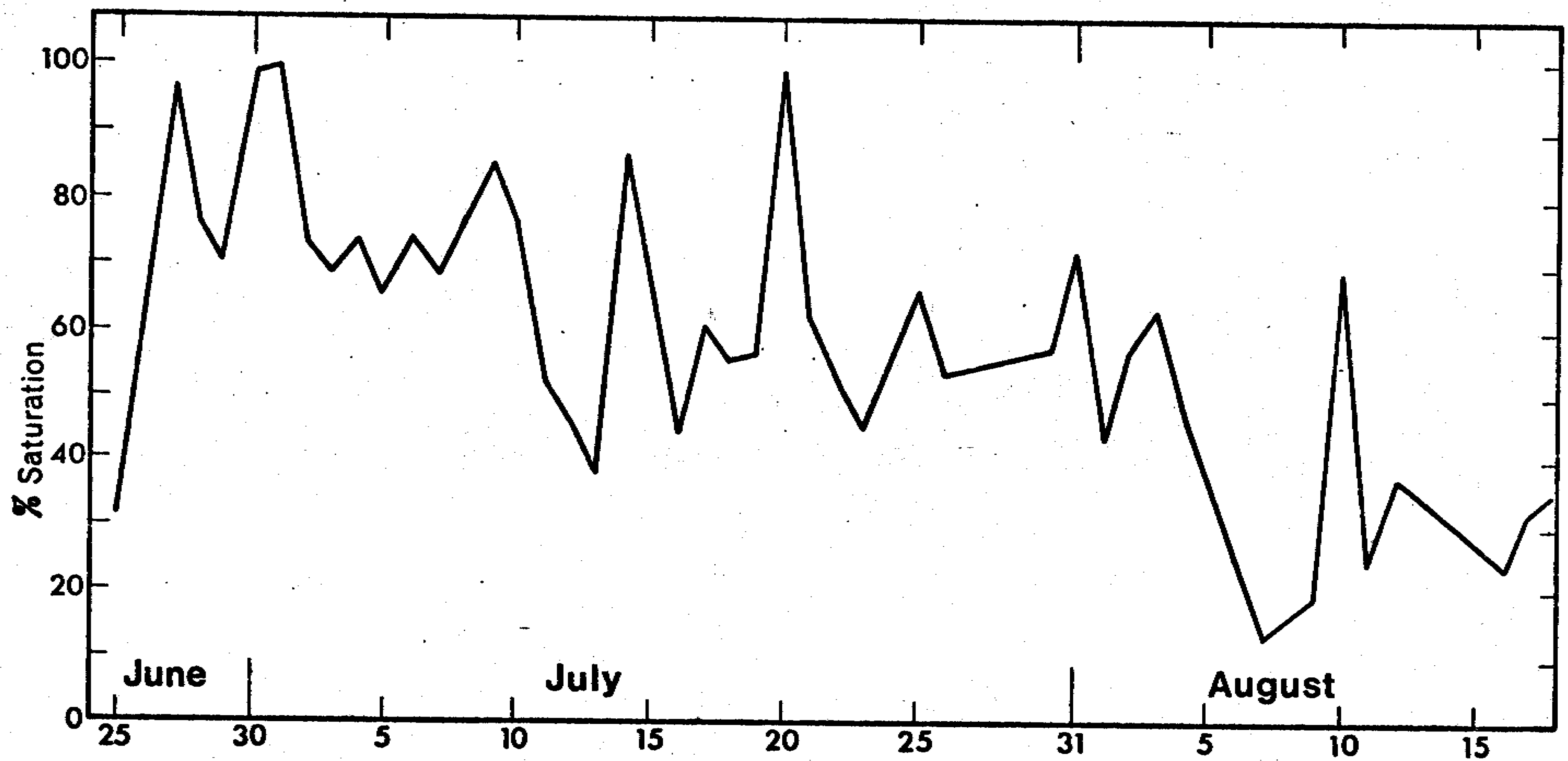

FIGURE 9

NET RADIATION - OBSERVED AND PREDICTED

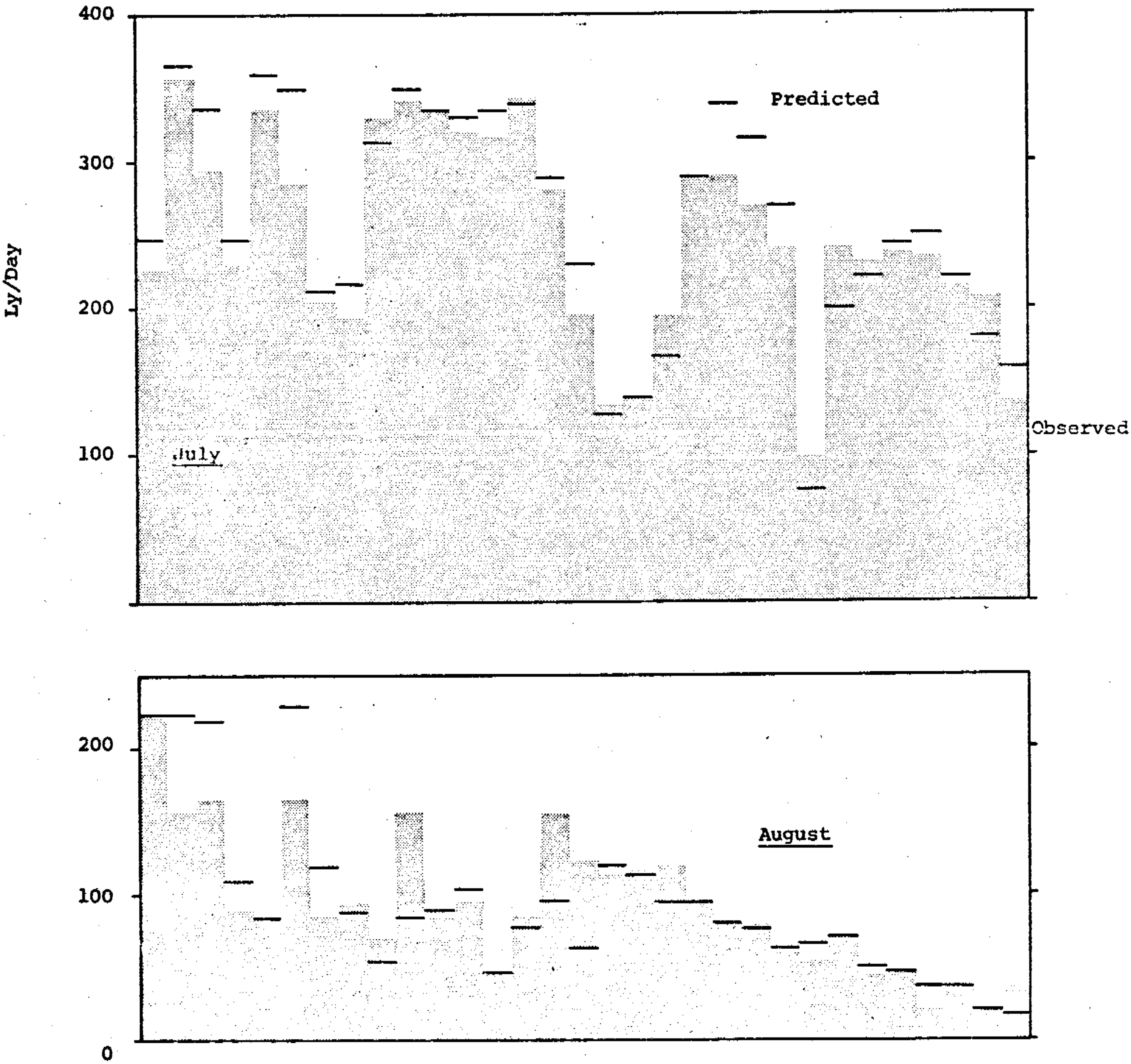

b

TABLE 1

VEGETATION CHARACTERISTICS OF TWO MICROCLIMATIC SITES*

Site	Species	% Frequency	% Cover
1	Carex stans	100	28.7
	Salix arctica	75	1.6
	Pedicularis sudetica	58	.9
	Saxifraga hirculus	16	.1
	Cardamine digitata	8	.1
			31.4
	Drepanocladus sp	100	90.8
	water	100	8.3
		TOTAL AVERAGE COVER	130.5
2	Salix arctica	100	12.0
	Poa arctica	100	5.5
	Stellaria longipes	91	1.2
	Dryas integrifolia	83	3.2
	Draba sp	58	.5
	Papaver radicatum	33	.3
	Saxifraga oppositifolia	25	.2
	Potentilla arctica	25	.2
	Pediculatis arctica	16	.1
	Melandrium apetalum ssp arcticum	8	.1
	Taraxacum sp	8	.1
	Ranunculus nivalis	8	.1
	Cerastium alpinum	8	.1
			23.6
	Mosses	100	8.0
	Litter	100	16.8
	Bare ground	100	51.3
		TOTAL AVERAGE COVER	99.7

* From Lambert (1974)

TABLE 2

SOIL PHYSICAL PROPERTIES

SITE	DEPTH (cm)	% GRAVEL	% SAND	% SILT-CLAY	% ORGANIC	% MOISTURE (Dry Weight)	BULK DENSITY (g/cm^3)
1	0-5	-	17.9	27.9	54.2	218-460	0.21
	5-10	-	16.7	56.7	26.6	65-228	0.66
	10-15	-	19.5	63.1	17.6	74-97	1.02
	15-20	-	17.5	61.8	20.8	70-104	0.98
	20-29	0.2	7.4	92.4	-	153.8	-
	30-300	-	-	Mostly Ice	-	-	-
2	0-5	5.2	45.7	29.8	12.4	22-48	1.12
	5-10	21.5	39.3	30.0	9.2	14-42	1.38
	10-15	18.6	49.7	24.9	6.3	13-32	1.55
	15-20	13.1	49.2	31.7	5.8	12-30	1.62
	20-25	28.5	42.9	23.4	5.2	10-29	1.64
	25-30	21.6	52.9	23.3	2.3	9-15	1.67
	30-35	18.9	58.8	13.0	4.6	12	1.77
	35-40	36.6	44.0	14.9	4.5	15	1.62
	60-80	0.1	13.6	86.3	-	77.4	1.09
	80-100	7.9	44.9	47.2	-	49.3	1.54
	100-110	7.9	28.9	63.2	-	168.6	0.73
	110-130	23.0	18.1	58.8	-	215.2	0.51
	130-140	27.3	16.0	56.8	-	249.6	0.45
	140-150	18.3	12.6	69.1	-	68.0	1.51
	150-160	18.9	16.1	64.9	-	177.4	0.57
	160-200	19.0	33.2	48.6	-	47.1	1.75
	200-240	13.3	25.1	61.6	-	17.5	2.51
	240-270	2.7	23.5	73.9	-	47.0	1.33
	270-280	0.3	18.8	80.9	-	53.4	1.20
	280-291	-	12.1	87.9	-	53.8	1.17
	291-302	-	8.9	91.1	-	53.4	1.35
	303-313	-	8.3	91.8	-	46.5	1.21

TABLE 3

INPUT DATA FOR SITE 1

LAYER	DEPTH (cm)	THERMAL CONDUCTIVITY* Frozen	Unfrozen	HEAT CAPACITY** Frozen	Unfrozen
Organic	0-10	1.18	2.90	1.97	4.20
Silt-Clay	10-30	30.7	8.40	1.92	3.86
Ice	30 →	22.3	5.46	1.89	4.20

Snow density (measured) = 0.34 g/cm^3

Snow albedo (maximum value) = 0.82

Surface albedo (measured) = 0.18

Snow roughness (from Weller 1974) = 0.03 cm

Surface roughness (from Weller 1974) = 2.00 cm

* cgs units

** $J/g/^{o}C$

TABLE 4

INPUT DATA FOR SITE 2

LAYER	DEPTH (cm)	THERMAL CONDUCTIVITY Frozen	Unfrozen	HEAT CAPACITY Frozen	Unfrozen
Organic-Silt-Sand	0-10	13.4	7.56	2.27	2.94
Silt-Sand	10-60	11.8	11.8	2.35	2.77
Icy Silt	60 →	33.6	10.5	2.10	3.78

Other data same as Table 3.

FIGURE 4

RECORDING SYSTEM